Original Article

Magnetic resonance imaging study of normal cranial bone marrow conversion at high altitude

Haihua Bao[#], Xin He[#^], Xiaoguang Li, Yuntai Cao[^], Naihui Zhang[^]

Department of Medical Imaging Center, Qinghai University Affiliated Hospital, Xining, China

Contributions: (I) Conception and design: H Bao, X He; (II) Administrative support: H Bao; (III) Provision of study materials or patients: X Li; (IV) Collection and assembly of data: H Bao, X Li, X He; (V) Data analysis and interpretation: X Li, X He; (VI) Manuscript writing: All authors; (VII) Final approval of manuscript: All authors.

[#]These authors contributed equally to this work.

Correspondence to: Haihua Bao. Department of Medical Imaging Center, Qinghai University Affiliated Hospital, 29 Tongren Road, Xining 810000, China. Email: baohelen2@sina.com.

Background: To use conventional magnetic resonance imaging (MRI) and diffusion-weighted imaging (DWI) to investigate the effects of long-term hypoxia on cranial bone marrow conversion in healthy people at high altitudes.

Methods: A total of 1,130 individuals were selected from altitudinal areas of 2,000–3,000, 3,100–4,000, and >4,100 m. Each altitude range was divided into 5 age groups: 0–5, 6–14, 15–29, 30–49, and ≥50 years. Firstly, cranial bone marrow typing of the participants in each altitude range was performed on sagittal T1-weighted images (T1WI) according to the average diploe thickness and signal intensity of the normal skull, and the relationship between bone marrow conversion and age was analyzed. Secondly, the apparent diffusion coefficient (ADC) values of the frontal bone, parietal bone, occipital bone, and temporal bone were measured in the DWI post-processing workstation and statistical methods were used to analyze whether different altitudinal gradients and long-term hypoxic environment had any effect on cranial bone marrow conversion.

Results: There was a positive correlation between bone marrow type and age in the healthy populations at all 3 levels of altitude ($P<0.05$). The average thickness of the cranial diploe also positively correlated with age ($P<0.05$); in the age ranges of 30–49 and ≥50 years, the ADC values of the occipital and temporal bone marrow positively correlated with increasing altitude ($P<0.05$).

Conclusions: The cranial bone marrow of normal people at high altitudes changes from Type I to Type IV with increasing age and under the influence of long-term chronic hypoxia. The bone marrow of the occipital and temporal bones of healthy people aged 30–49 and ≥50 years showed erythromedularization during the process of Type III and IV bone marrow conversion.

Keywords: Bone marrow erythromedularization; cranial bone marrow; high altitude; magnetic resonance imaging

Submitted Jul 19, 2021. Accepted for publication Mar 11, 2022.
doi: 10.21037/qims-21-740
View this article at: https://dx.doi.org/10.21037/qims-21-740

^ ORCID: Xin He, 0000-0002-7146-3411; Yuntai Cao, 0000-0002-1747-4232; Naihui Zhang, 0000-0002-3555-6098.

© Quantitative Imaging in Medicine and Surgery. All rights reserved.

Introduction

In the human hematopoietic system, red bone marrow is the primary tissue and gradually transforms into yellow bone marrow with age (1). The hematopoietic system is dynamic and adaptively adjusts when the body experiences hematological malignancies, bone metastasis of malignant tumors, severe anemia, long-term hypoxia, and bone marrow injury (2-4). When living at high altitude, humans are challenged with a unique environment in which hypoxia is a severe problem. Due to low atmospheric pressure and oxygen partial pressure, long-term hypoxia will stimulate the kidneys, increasing the secretion of erythropoietin (EPO), which then stimulates the production of erythroid cells, resulting in an increase of bone marrow erythrocytes that is reflected by increased hematocrit and decreased oxyhemoglobin saturation (5). Negative feedback regulation prevents overproduction of EPO (5). The EPO is affected by hypoxia, anemia, hormone levels, smoking, and other factors, among which hypoxia is the most influential factor. Regulation of the human hematopoietic system in high-altitude areas is an essential adaptation for survival (6-8).

The ability of conventional magnetic resonance imaging (MRI) to detect patterns of bone marrow changes in the early stages of cranial bone marrow disease is limited when the only change is the composition of intracellular free water within the bone marrow and the content of the various cells within the bone marrow remains unchanged. Combining MRI and diffusion-weighted imaging (DWI) makes it possible to conduct a comprehensive investigation and determination of normal MRI features at different altitudes and anatomic sites.

There are a few reports on MRI studies examining the appearance of normal cranial bone marrow (9-14); to our knowledge, from the perspective of imaging, the relationship between cranial bone marrow typing and age of normal residents at high altitudes has not been reported. In this study we used a non-invasive MRI method to explore the normal development of cranial bone marrow at high altitude and the effect of long-term hypoxia on the conversion of red and yellow bone marrow in normal people. The aim of the study was to clarify the development of normal cranial bone marrow and provide insight regarding the invasion of malignant tumors, malignant hematologic disease, lymphoma, multiple myeloma, and other diseases, thus assisting the early treatment of the disease. At the same time, we also wanted to provide reference values for the occurrence and development of bone marrow disease in the high-altitude hypoxic environment. We present the following article in accordance with the STROBE reporting checklist (available at https://qims.amegroups.com/article/view/10.21037/qims-21-740/rc).

Methods

Participants

Patients who underwent a craniocerebral MRI examination between 2016 and 2019 were selected as participants. The inclusion criteria were as follows: (I) normal cranial bone development with no abnormal findings on conventional head MRI; (II) normal laboratory examinations (including blood count and clotting time test); (III) normal neurological examination. The exclusion criteria were as follows: (I) history of traumatic brain injury or hematologic diseases; (II) history of malignant tumor; (III) any organic disease. A total 1,130 healthy Han Chinese residents aged from 8 months to 71 years (560 female, 570 male), with a median age of 24 years, were selected from areas with elevations of 2,000–3,000, 3,100–4,000, and >4,100 m. Each altitude range was divided into 5 age groups: 0–5, 6–14, 15–29, 30–49, and ≥50 years. The number of participants in each age group at the altitude of 2,000–3,000 m was 80, 100, 100, 100, and 80 respectively; 60, 80, 80, 80, and 60 respectively at the altitude of 3,100–4,000 m; and 50, 70, 70, 70, and 50 respectively at >4,100 m. The grouping principle was based on prior studies with consideration of children's developmental characteristics, because childhood is the period with the fastest bone development, the younger groups had a smaller age-span, and the older groups has larger age-spans because bone development gradually slows with age (15-21).

Data acquisition

All imaging was performed on a 3.0T Philips Achieva TX scanner (Philips Medical Systems, Eindhoven, Netherlands) with an 8-channel head coil.

MRI protocols

Sagittal T1-weighted image (T1WI) scan parameters were as follows: repetition time/echo time (TR/TE) =127.00/1.87 ms, slice thickness =6.0 mm (6.0 mm gap), imaging matrix =200×230, flip angle =30°, field of view (FOV) =125–260 mm, scan time: 128 seconds. The DWI imaging parameters were

© Quantitative Imaging in Medicine and Surgery. All rights reserved.

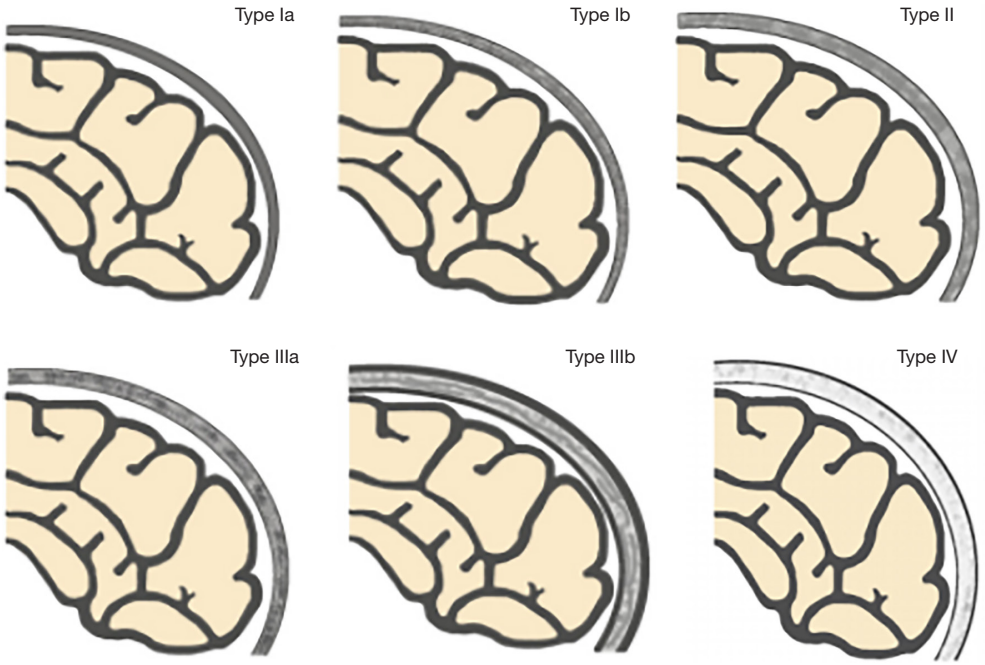

Figure 1 Schematic of the patterns of normal cranial bone marrow (4-type 6-subtype system): Types Ia–IV. [Source of the picture: Li Q, Pan SN, Yin YM, Li W, Chen ZA, Liu YH, *et al.* (22)].

as follows: using spin echo-echo planar imaging (SE-EPI) sequence, apparent diffusion coefficient (ADC) maps were generated using DWIs with b values of 0 and 1,000 s/mm^2, TR/TE =2,380/90 ms, slice thickness =6 mm (6 mm gap), imaging matrix =152×121, FOV =125–260 mm, number of signals averaged (NSA) =3 times, scan time: 28 s.

Image analysis

The Extended Magnetic Resonance Workspace (Philips) was used for image processing, and image analysis was performed by 2 experienced radiologists with >15 years of diagnostic experience. They were blinded to the participant's age, gender, and other relevant clinical information, and the images were independently interpreted. Any disagreement between the 2 readers was resolved by discussion with a third reader, who was also an experienced radiologist.

Based on the research results of Okada *et al.* (9), Ricci *et al.* (10), and Li *et al.* (22), we used a "4-type 6-subtype system" of cranial bone marrow patterns (*Figure 1*) to classify the skull on sagittal T1WI. The classification is based on the following criteria: (I) average thickness of each cranial diploe (average values of frontal, parietal, occipital, and temporal diploes); (II) difference in thickness of each cranial diploe (including frontal bone, parietal bone, occipital bone, and temporal bone); (III) difference in cranial bone marrow signal intensity (with reference to genioglossus muscle at the same level); (IV) multidimensional analysis combining sagittal T1WI images with axial T1WI images for cranial bone MRI pattern analysis.

The types/subtypes were classified as follows:

- Type Ia: each cranial diploe is relatively thin, only internal occipital protuberance is slightly thicker, and the MRI shows uniformly low to medium signal intensity.
- Type Ib: morphology of the cranial bone is similar to that of Type Ia, but its low–medium signal intensity is accompanied by scattered, speckled high signal intensity.
- Type II: each cranial diploe is slightly thickened, mainly occipital thickening, low signal intensity cranial bone marrow has scattered small, patchy high signal intensity.
- Type IIIa: each cranial diploe is further thickened, and the cranial bone marrow shows medium–high signal intensity.
- Type IIIb: cranial diploe obviously thickened,

© Quantitative Imaging in Medicine and Surgery. All rights reserved.

especially in the occipital bone, manifesting as high signal intensity cranial bone marrow with scattered, ill-defined, patchy low signal intensity.

- ❖ Type IV: obvious thickening of the cranial bone and uniformly high signal intensity in the cranial diploe, with some scattered, patchy low signal intensity areas.

Quantitative analysis of the ADC values of cranial bone marrow was measured with DWI post-processing software. Bone marrow that was slightly thinner than the thicker parts of the frontal, parietal, occipital, and temporal diploes was selected in the regions of interest (ROIs) to avoid a partial volume effect. The ROIs were defined as 15–20 mm^3 and in them the left and right parietal, frontal, occipital, and temporal bone marrow of each participant were selected to measure the ADC values. The average ADC value of the same cranial bone marrow was calculated 3 times.

Statistical analysis

The software SPSS 19.0 (IBM Corp., Chicago, IL, USA) was used for statistical analysis. Enumeration data were analyzed by chi-square test, and measurement data were analyzed by variance analysis. The ADC values of each participant's different cranial bone marrows were measured to perform analysis of variance (ANOVA).

Ethical statement

The study was conducted in accordance with the Declaration of Helsinki (as revised in 2013). The study was approved by the Ethics Committee of Qinghai University Affiliated Hospital and individual consent for this retrospective analysis was waived.

Results

Correlation between MRI typing of cranial bone marrow and age in healthy populations at high altitude

Tables 1-3 and *Figures 2-4* show the number of cases for each type of bone marrow, and the average thickness of the cranial diploe in each age range at the 3 altitudes. There was a positive correlation between cranial bone marrow typing and age in the normal populations at these altitudes, and the average thickness of cranial diploe positively correlated with age ($P<0.05$); that is, the cranial bone marrow pattern of the normal populations at high altitude changed from Type I to Type IV with age.

Correlation between altitude and cranial bone marrow ADC values

There was no significant difference between altitude and cranial bone marrow ADC values in the 0–5, 6–14, and 15–29 years age groups ($P>0.05$). In the age ranges of 30–49 and ≥50 years, the ADC values of the occipital and temporal bones increased gradually with increasing altitude ($P<0.05$), but there was no significant difference in the parietal and frontal bones ($P>0.05$) (*Tables 4-8*, *Figures 5,6*).

Discussion

Our study of normal cranial bone marrow conversion at high altitude showed that the effect of a hypoxic environment becomes more severe with increasing altitude, and the ADC values of the occipital and temporal bone marrow of healthy Han Chinese residents aged 30–49 and ≥50 years tended to increase; that is, the restriction degree on the diffusion of water molecules reduced. Considering the influence of a long-term chronic hypoxic environment, the occipital and temporal bone marrow of healthy Han Chinese residents in these age groups showed erythromedularization during Types III and IV bone marrow conversion, which may be related to increased bone marrow erythrocytes caused by long-term hypoxic stimulation of the kidney to produce EPO. Therefore, using DWI technology, ADC values can be used to indirectly reflect changes in the water and fat content of bone marrow during conversion and obtain reference ranges of ADC values of normal cranial bone marrow at different ages. In addition, DWI can be used in further qualitative and quantitative analysis of the proportion of red and yellow bone marrow in different age groups, to assist in the diagnosis of cranial bone marrow lesions.

Okada *et al.* first proposed that the MRI characteristics of healthy cranial bone marrow were age-related (9), and Ricci *et al.* suggested a 3-type 3-subtype system to classify the MRI patterns in normal cranial bone marrow based on the conversion patterns (10), setting the foundation for studying cranial bone marrow using MRI. Li *et al.* (22) put forward the 4-type 6-subtype system to assess the MRI patterns of cranial bone marrow developmental changes at different ages, a further development of the study of cranial bone marrow using MRI.

There is abundant bone marrow in the medulla of the

© Quantitative Imaging in Medicine and Surgery. All rights reserved.

Table 1 Relationship between normal cranial bone marrow typing and age at 2,000–3,000 m above sea level

Age group (years)	Bone marrow type, n (%)						Diploe thickness (mm)
	Ia	Ib	II	IIIa	IIIb	IV	
0–5	26 (32.5)	34 (42.5)	20 (25.0)	0 (0.0)	0 (0.0)	0 (0.0)	1.72±0.69
6–14	2 (2.0)	16 (16.0)	39 (39.0)	6 (6.0)	37 (37.0)	0 (0.0)	2.75±0.93
15–29	0 (0.0)	0 (0.0)	7 (7.0)	7 (7.0)	66 (66.0)	20 (20.0)	3.86±0.85
30–49	0 (0.0)	0 (0.0)	5 (5.0)	9 (9.0)	71 (71.0)	15 (15.0)	4.12±1.20
≥50	0 (0.0)	0 (0.0)	0 (0.0)	11 (13.8)	20 (25.0)	49 (61.3)	4.34±1.00
χ^2/F (P)	481.638 (0.000)						113.039 (0.000)
r (P)	0.739 (0.000)						0.673 (0.000)

Table 2 Relationship between normal cranial bone marrow typing and age at 3,100–4,000 m above sea level

Age group (years)	Bone marrow type, n (%)						Diploe thickness (mm)
	Ia	Ib	II	IIIa	IIIb	IV	
0–5	20 (33.3)	29 (48.3)	11 (18.3)	0 (0.0)	0 (0.0)	0 (0.0)	1.85±0.67
6–14	5 (6.3)	15 (18.8)	40 (50.0)	4 (5.0)	16 (20.0)	0 (0.0)	2.88±0.99
15–29	0 (0.0)	0 (0.0)	9 (11.3)	4 (5.0)	58 (72.5)	9 (11.3)	3.87±1.02
30–49	0 (0.0)	0 (0.0)	6 (7.5)	8 (10.0)	60 (75.0)	6 (7.5)	3.93±0.91
≥50	0 (0.0)	0 (0.0)	0 (0.0)	10 (16.7)	13 (21.7)	37 (61.7)	4.31±0.89
χ^2/F (P)	441.959 (0.000)						76.104 (0.000)
r (P)	0.772 (0.000)						0.635 (0.000)

Table 3 Relationship between normal cranial bone marrow typing and age at an altitude >4,100 m

Age group (years)	Bone marrow type, n (%)						Diploe thickness (mm)
	Ia	Ib	II	IIIa	IIIb	IV	
0–5	21 (42.0)	22 (44.0)	7 (14.0)	0 (0.0)	0 (0.0)	0 (0.0)	1.80±0.59
6–14	5 (7.1)	16 (22.9)	33 (47.1)	4 (5.7)	12 (17.1)	0 (0.0)	2.79±0.85
15–29	0 (0.0)	0 (0.0)	13 (18.6)	9 (12.9)	44 (62.9)	4 (5.7)	3.67±0.87
30–49	0 (0.0)	0 (0.0)	9 (12.9)	8 (11.4)	47 (67.1)	6 (8.6)	3.68±1.00
≥50	0 (0.0)	0 (0.0)	3 (6.0)	6 (12.0)	15 (30.0)	26 (52.0)	4.32±0.90
χ^2/F (P)	335.266 (0.000)						67.750 (0.000)
r (P)	0.758 (0.000)						0.646 (0.000)

diaphysis, flat bones, and irregular bones (23). Red bone marrow and yellow bone marrow are mixed in the cavitas medullaris, where the red bone marrow produces blood cells and has a hematopoietic function, thus is more active, and the proportion of water molecules is higher, followed by the proportions of fat and protein; yellow bone marrow is relatively inactive and contains more fat, followed by water molecules and protein (24). The conversion of normal red and yellow bone marrow is regular, meaning that from infancy to adulthood, the process of bone marrow

© Quantitative Imaging in Medicine and Surgery. All rights reserved.

Figure 2 MRI patterns of normal cranial bone marrow (4-type 6-subtype system) represented respectively as Types Ia–IV, at the altitude of 2,000–3,000 m. MRI, magnetic resonance imaging.

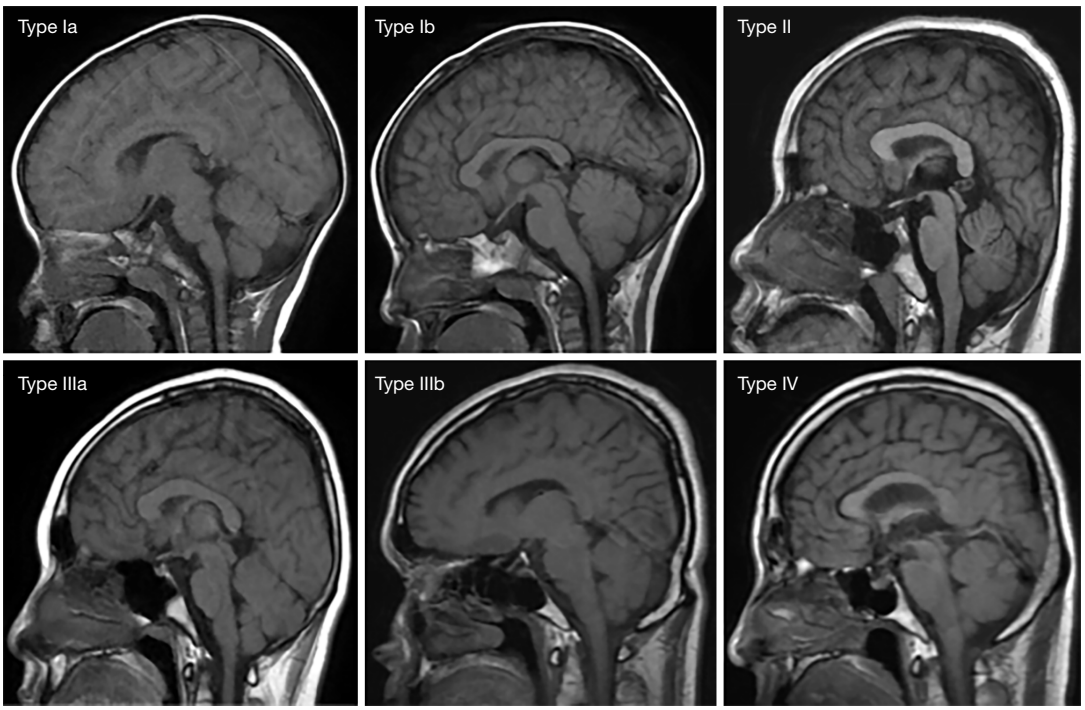

Figure 3 MRI patterns of normal cranial bone marrow (4-type 6-subtype system) represented respectively as Types Ia–IV, at the altitude of 3,100–4,000 m. MRI, magnetic resonance imaging.

© Quantitative Imaging in Medicine and Surgery. All rights reserved.

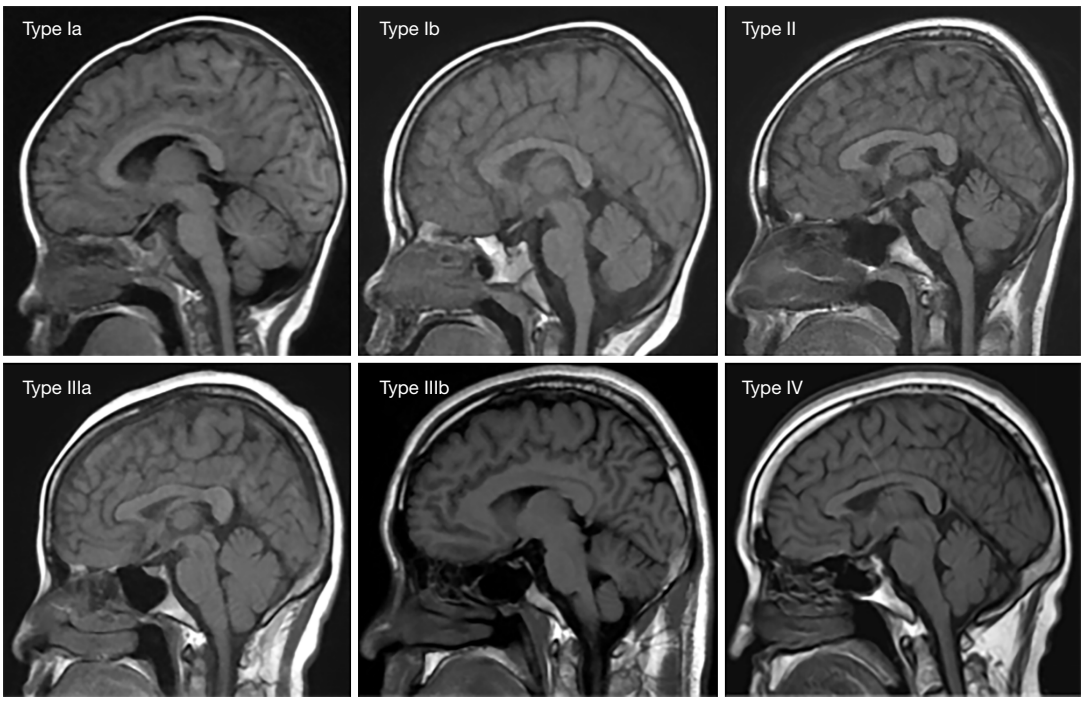

Figure 4 MRI patterns of normal cranial bone marrow (4-type 6-subtype system) represented respectively as Types Ia–IV, at the altitude of >4,100 m. MRI, magnetic resonance imaging.

Table 4 ADC values of cranial bone marrow at different elevations in the age range of 0–5 years

Altitude range (m)	n	ADC values ($\times10^{-3}$ mm^2/s)			
		Parietal bone	Occipital bone	Frontal bone	Temporal bone
2,000–3,000	80	1.02±0.21	1.27±0.24	0.96±0.27	1.18±0.22
3,100–4,000	60	0.95±0.25	1.26±0.26	1.05±0.25	1.16±0.22
≥4,100	50	0.97±0.24	1.29±0.27	0.98±0.23	1.18±0.23
F (P)		1.824 (0.164)	0.137 (0.872)	1.932 (0.148)	0.251 (0.779)
r (P)		−0.125 (0.086)	0.025 (0.732)	0.021 (0.778)	−0.006 (0.933)

ADC, apparent diffusion coefficient.

Table 5 ADC values of cranial bone marrow at different elevations in the age range of 6–14 years

Altitude range (m)	n	ADC values ($\times10^{-3}$ mm^2/s)			
		Parietal bone	Occipital bone	Frontal bone	Temporal bone
2,000–3,000	100	0.97±0.28	1.07±0.25	1.01±0.23	1.02±0.26
3,100–4,000	80	0.92±0.25	1.02±0.24	1.02±0.29	1.01±0.24
≥4,100	70	0.89±0.29	1.02±0.27	1.01±0.24	1.04±0.25
F (P)		1.798 (0.168)	1.108 (0.332)	0.031 (0.969)	0.192 (0.826)
r (P)		−0.100 (0.115)	−0.070 (0.267)	−0.010 (0.875)	−0.023 (0.722)

ADC, apparent diffusion coefficient.

© Quantitative Imaging in Medicine and Surgery. All rights reserved.

Table 6 ADC values of cranial bone marrow at different elevations in the age range of 15–29 years

Altitude range (m)	n	ADC values ($\times10^{-3}$ mm^2/s)			
		Parietal bone	Occipital bone	Frontal bone	Temporal bone
2,000–3,000	100	0.62±0.23	0.64±0.25	1.00±0.26	1.00±0.23
3,100–4,000	80	0.66±0.24	0.68±0.22	1.00±0.22	1.05±0.25
≥4,100	70	0.69±0.26	0.67±0.24	1.05±0.24	1.05±0.26
F (P)		1.608 (0.202)	0.527 (0.591)	0.989 (0.373)	1.003 (0.368)
r (P)		0.088 (0.166)	0.045 (0.481)	0.083 (0.192)	0.089 (0.161)

ADC, apparent diffusion coefficient.

Table 7 ADC values of cranial bone marrow at different elevations in the age range of 30–49 years

Altitude range (m)	n	ADC values ($\times10^{-3}$ mm^2/s)			
		Parietal bone	Occipital bone	Frontal bone	Temporal bone
2,000–3,000	100	1.00±0.24	0.57±0.24	1.01±0.23	0.57±0.19
3,100–4,000	80	1.02±0.25	0.65±0.23	0.99±0.24	0.61±0.27
≥4,100	70	1.03±0.27	0.69±0.26	0.98±0.24	0.70±0.28
F (P)		0.417 (0.659)	5.038 (0.007)	0.229 (0.796)	5.920 (0.003)
r (P)		0.084 (0.184)	0.175 (0.006)	–0.046 (0.466)	0.179 (0.005)

ADC, apparent diffusion coefficient.

Table 8 ADC values of cranial bone marrow at different elevations in the age range of ≥50 years

Altitude range (m)	n	ADC values ($\times10^{-3}$ mm^2/s)			
		Parietal bone	Occipital bone	Frontal bone	Temporal bone
2,000–3,000	80	0.97±0.25	0.53±0.21	1.03±0.25	0.52±0.21
3,100–4,000	60	0.97±0.24	0.56±0.20	1.00±0.24	0.57±0.27
≥4,100	50	0.99±0.26	0.64±0.21	0.95±0.27	0.65±0.27
F (P)		0.075 (0.928)	4.636 (0.011)	1.517 (0.222)	4.414 (0.013)
r (P)		0.014 (0.851)	0.188 (0.009)	-0.111 (0.127)	0.182 (0.012)

ADC, apparent diffusion coefficient.

conversion of the axial skeleton is gradual and continues throughout adulthood, with the proportion of red bone marrow gradually decreasing, and the proportion of yellow bone marrow gradually increasing (25-27). From an imaging perspective, bone marrow shows different signal intensities on MRI due to the differing content of water, fat, and other components. In infancy, the predominant bone marrow is red, and the water content is higher than that of fat, thus cranial bone marrow shows a relatively low signal on T1WI images. With increasing age, red bone marrow gradually converts to yellow bone marrow, and the fat content gradually increases (1). The T1WI images show a relatively high signal intensity of cranial bone marrow. The signal intensity pairs of red and yellow bone marrow are relatively more obvious on T1WI images compared with T2WI images, so T1WI images are usually chosen for cranial bone marrow typing (24).

The composition of bone marrow also varies with anatomic location (28,29). The peak of the conversion from red bone marrow to yellow bone marrow happens

© Quantitative Imaging in Medicine and Surgery. All rights reserved.

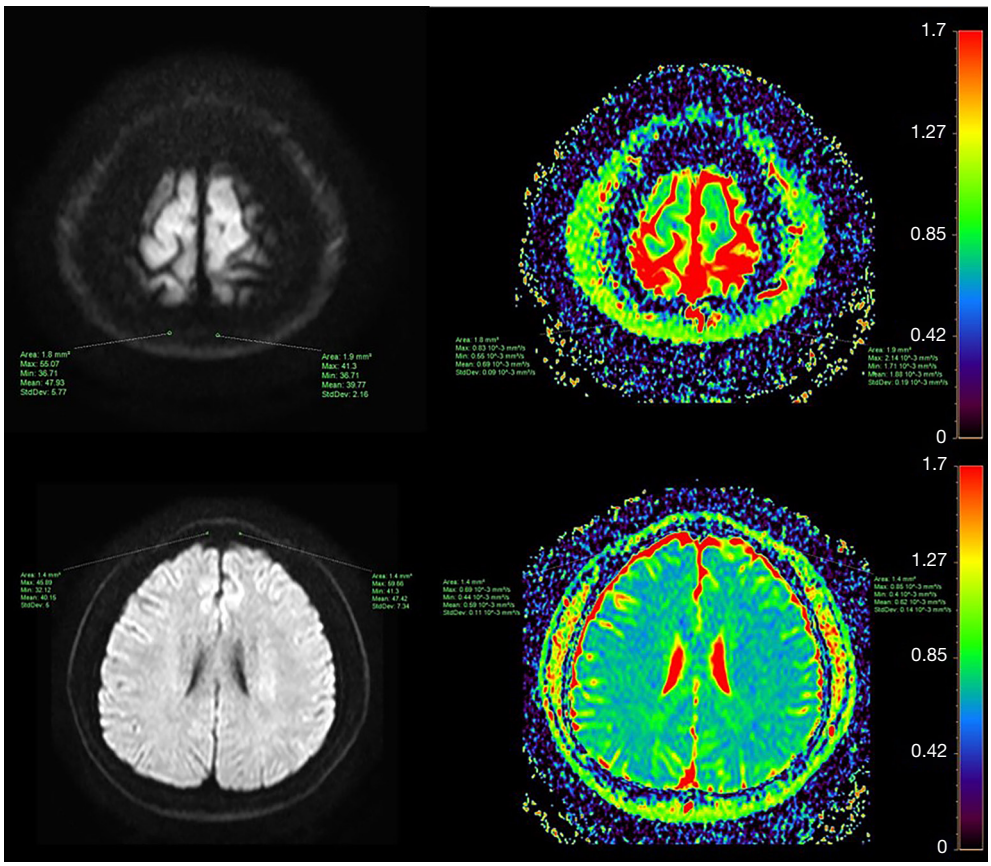

Figure 5 ADC measurement of ROI in parietal and frontal bone marrow of a 30-year-old male. ADC, apparent diffusion coefficient; ROI, region of interest.

in the 1st–2nd decades and the 7th decade, but the rate of conversion varies in the specific areas of the axial or appendicular skeleton. In addition, the conversion rate also differs in different regions of a single bone, and it is considered that factors affecting conversion include local temperature, vascularity, and oxygen partial pressure. Mosavi *et al.* believe that human development is accompanied by changes in water and fat content in the bone marrow and that MRI can reflect the relationship between bone marrow conversion and age (30). Ricci *et al.* put forward the initial classification of cranial bone marrow (10); that is, Type I shows relatively low signal intensity in bone marrow, with only some scattered speckled high signal intensity in the frontal and occipital bone marrows, and is mainly seen in children under 10 years old; Type II has a relatively uniform high signal intensity in the cranial bone marrow, with only the parietal bone showing scattered patchy high signal intensity. Type III has a widely consistent high signal intensity in the cranial bone marrow. Both Types II and III can be seen in every age group. On this basis, Li *et al.* (22) used a "4-type 6-subtype system" to classify cranial bone marrow, which has proven to be a valuable tool for the study of normal cranial development, bone marrow typing, and bone marrow lesions.

Because osteomuscular system diseases and bone metastases of malignant tumors mostly occur in the spine, femur, and pelvis, there have been more bone marrow studies on these bones (31,32), and relatively few MRI studies of cranial bone marrow. When skull invasion is suspected, conventional MRI combined with DWI technology can be used for auxiliary diagnosis. The DWI imaging technology is different from traditional MRI technology; its imaging basis is to detect whether the diffusion direction and degree of water molecules in the human body are limited, which enables tissue imaging comparison (33). Red bone marrow and yellow bone marrow are mixed together in the cavitas medullaris. There are more water molecules in red bone marrow and more fat

© Quantitative Imaging in Medicine and Surgery. All rights reserved.

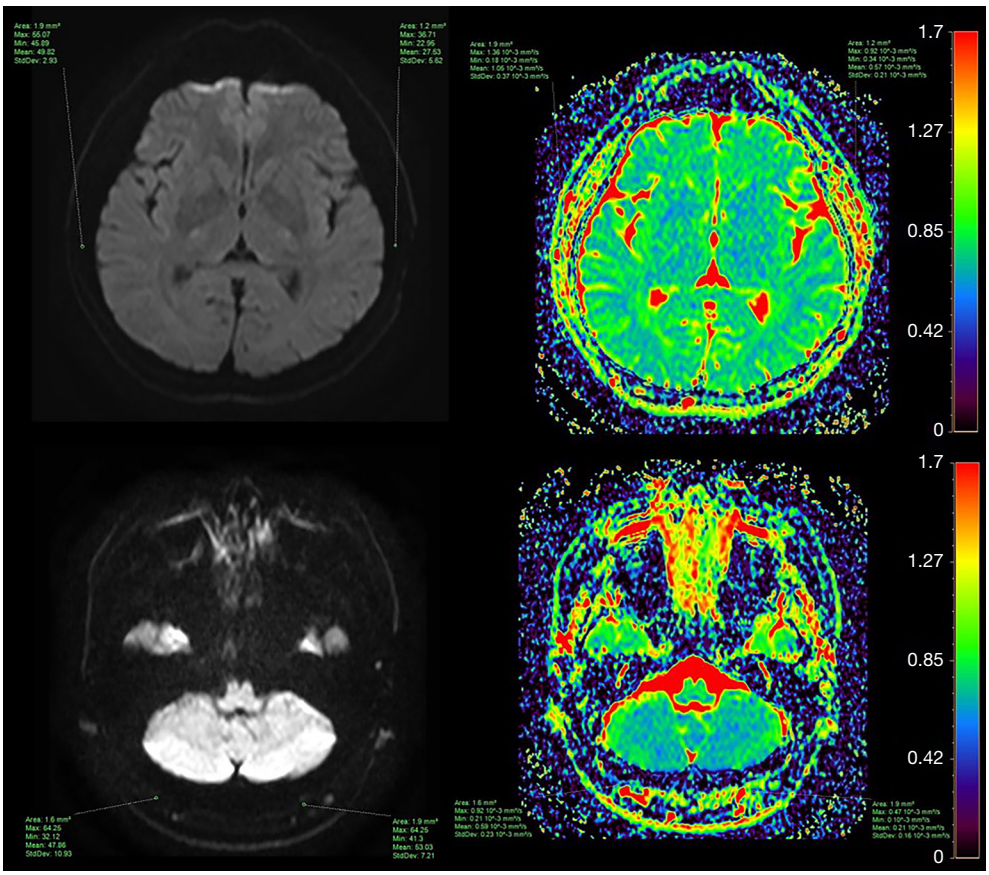

Figure 6 ADC measurement of ROI in temporal and occipital bone marrow of a 30-year-old male. ADC, apparent diffusion coefficient; ROI, region of interest.

in yellow bone marrow. When the proportion of red bone marrow is high, there will be more water molecules and their movement is not restricted, so the ADC values are relatively high. In contrast, when the proportion of yellow bone marrow is high, there will be high fat content, the diffusion of water molecules is limited, and the ADC values are relatively low.

Study limitations

First, because the characteristic clival bone marrow is relatively small compared with cranial bone marrow, we did not perform an MRI study of the clival bone marrow. Second, the grouping principle in this study was based on the characteristics of children's development. However, there were fewer cases in the 0–15 age range; the age interval grouping should be further improved to ensure greater accuracy. Due to a limitation of regional factors, we did not compare the bone marrow conversion in healthy skulls at low altitude. Third, because the thickness of the cranial diploe is thinner than that of the spine, pelvis, and femur, the average ADC value of the cranial bone marrow needs to be measured many times, which will cause measurement error during scanning, so the sample size was relatively larger in this study to reduce this error.

Conclusions

Under the influence of low pressure, hypoxia, and low temperature at high altitudes, the human hematopoietic system will produce a stress response to meet the survival needs in this environment. The bone marrow of the occipital bone and temporal bone of healthy people aged 30–49 years old and ≥50 years old changes in a process of Types III and IV bone marrow conversion; that is, the bone marrow tissue of residents in high-altitude areas will

© Quantitative Imaging in Medicine and Surgery. All rights reserved.

show changes due to long-term residence in a hypoxic environment.

Acknowledgments

Funding: This study was supported by the Key Specialized Program of Medical Imaging in Qinghai Province (No. 2020-1301).

Footnote

Reporting Checklist: The authors have completed the STROBE reporting checklist. Available at https://qims.amegroups.com/article/view/10.21037/qims-21-740/rc

Conflicts of Interest: All authors have completed the ICMJE uniform disclosure form (available at https://qims.amegroups.com/article/view/10.21037/qims-21-740/coif). The authors have no conflicts of interest to declare.

Ethical Statement: The authors are accountable for all aspects of the work in ensuring that questions related to the accuracy or integrity of any part of the work are appropriately investigated and resolved. The study was conducted in accordance with the Declaration of Helsinki (as revised in 2013). The study was approved by Ethics Committee of Qinghai University Affiliated Hospital and individual consent for this retrospective analysis was waived.

Open Access Statement: This is an Open Access article distributed in accordance with the Creative Commons Attribution-NonCommercial-NoDerivs 4.0 International License (CC BY-NC-ND 4.0), which permits the non-commercial replication and distribution of the article with the strict proviso that no changes or edits are made and the original work is properly cited (including links to both the formal publication through the relevant DOI and the license). See: https://creativecommons.org/licenses/by-nc-nd/4.0/.

References

1. Gurevitch O, Slavin S, Feldman AG. Conversion of red bone marrow into yellow - Cause and mechanisms. Med Hypotheses 2007;69:531-6.
2. Nishii T, Kono AK, Akasaka Y, Mori T, Hayakawa A, Iijima K, Sugimura K. Bone marrow magnetic resonance imaging of the clivus in pediatric leukemia patients and normal controls. Jpn J Radiol 2015;33:146-52.
3. Cao W, Liang C, Gen Y, Wang C, Zhao C, Sun L. Role of diffusion-weighted imaging for detecting bone marrow infiltration in skull in children with acute lymphoblastic leukemia. Diagn Interv Radiol 2016;22:580-6.
4. Wu TL, Byun NE, Wang F, Mishra A, Janve VA, Chen LM, Gore JC. Longitudinal assessment of recovery after spinal cord injury with behavioral measures and diffusion, quantitative magnetization transfer and functional magnetic resonance imaging. NMR Biomed 2020;33:e4216.
5. Wilber RL, Stray-Gundersen J, Levine BD. Effect of hypoxic "dose" on physiological responses and sea-level performance. Med Sci Sports Exerc 2007;39:1590-9.
6. Tymko MM, Tremblay JC, Bailey DM, Green DJ, Ainslie PN. The impact of hypoxaemia on vascular function in lowlanders and high altitude indigenous populations. J Physiol 2019;597:5759-76.
7. Köhler D, Dellweg D. Polycythemia. Deutsche medizinische Wochenschrift (1946) 2010;135:2300-3.
8. Bilo G, Caravita S, Torlasco C, Parati G. Blood pressure at high altitude: physiology and clinical implications. Kardiol Pol 2019;77:596-603.
9. Okada Y, Aoki S, Barkovich AJ, Nishimura K, Norman D, Kjos BO, Brasch RC. Cranial bone marrow in children: assessment of normal development with MR imaging. Radiology 1989;171:161-4.
10. Ricci C, Cova M, Kang YS, Yang A, Rahmouni A, Scott WW Jr, Zerhouni EA. Normal age-related patterns of cellular and fatty bone marrow distribution in the axial skeleton: MR imaging study. Radiology 1990;177:83-8.
11. Hajek PC, Baker LL, Goobar JE, Sartoris DJ, Hesselink JR, Haghighi P, Resnick D. Focal fat deposition in axial bone marrow: MR characteristics. Radiology 1987;162:245-9.
12. Simonson TM, Kao SC. Normal childhood developmental patterns in skull bone marrow by MR imaging. Pediatr Radiol 1992;22:556-9.
13. Nemeth AJ, Henson JW, Mullins ME, Gonzalez RG, Schaefer PW. Improved detection of skull metastasis with diffusion-weighted MR imaging. AJNR Am J Neuroradiol 2007;28:1088-92.
14. Moon WJ, Lee MH, Chung EC. Diffusion-weighted imaging with sensitivity encoding (SENSE) for detecting cranial bone marrow metastases: comparison with T1-weighted images. Korean J Radiol 2007;8:185-91.
15. Waitches G, Zawin JK, Poznanski AK. Sequence and rate of bone marrow conversion in the femora of children as seen on MR imaging: are accepted standards accurate?

© Quantitative Imaging in Medicine and Surgery. All rights reserved.

AJR Am J Roentgenol 1994;162:1399-406.
16. Le Bihan DJ. Differentiation of benign versus pathologic compression fractures with diffusion-weighted MR imaging: a closer step toward the "holy grail" of tissue characterization? Radiology 1998;207:305-7.
17. Richardson ML, Patten RM. Age-related changes in marrow distribution in the shoulder: MR imaging findings. Radiology 1994;192:209-15.
18. Moore SG, Dawson KL. Red and yellow marrow in the femur: age-related changes in appearance at MR imaging. Radiology 1990;175:219-23.
19. Dawson KL, Moore SG, Rowland JM. Age-related marrow changes in the pelvis: MR and anatomic findings. Radiology 1992;183:47-51.
20. Taccone A, Oddone M, Occhi M, Dell'Acqua AD, Ciccone MA. MRI "road-map" of normal age-related bone marrow. I. Cranial bone and spine. Pediatr Radiol 1995;25:588-95.
21. Sebag GH, Dubois J, Tabet M, Bonato A, Lallemand D. Pediatric spinal bone marrow: assessment of normal age-related changes in the MRI appearance. Pediatr Radiol 1993;23:515-8.
22. Li Q, Pan SN, Yin YM, Li W, Chen ZA, Liu YH, Wu ZH, Guo QY. Normal cranial bone marrow MR imaging pattern with age-related ADC value distribution. Eur J Radiol 2011;80:471-7.
23. Tao Y, Song D, Zhang F, Ren S, Zhang H, Sun L. Transplantation of bone-marrow-derived mesenchymal stem cells into a murine model of immune thrombocytopenia. Blood Coagul Fibrinolysis 2017;28:596-601.
24. Chan BY, Gill KG, Rebsamen SL, Nguyen JC. MR Imaging of Pediatric Bone Marrow. Radiographics 2016;36:1911-30.
25. Pace E, MacKinnon AD, deSouza NM. Variation of the apparent diffusion coefficient of skull bone marrow by age group, pubertal status, and gender in a pediatric population. Acta Radiol 2020;61:1240-8.
26. Loevner LA, Tobey JD, Yousem DM, Sonners AI, Hsu WC. MR imaging characteristics of cranial bone marrow in adult patients with underlying systemic disorders compared with healthy control subjects. AJNR Am J Neuroradiol 2002;23:248-54.
27. Herrmann J, Krstin N, Schoennagel BP, Sornsakrin M, Derlin T, Busch JD, Petersen KU, Graessner J, Adam G, Habermann CR. Age-related distribution of vertebral bone-marrow diffusivity. Eur J Radiol 2012;81:4046-9.
28. Xing X, Zhang J, Chen Y, Zhao Q, Lang N, Yuan H. Application of monoexponential, biexponential, and stretched-exponential models of diffusion-weighted magnetic resonance imaging in the differential diagnosis of metastases and myeloma in the spine-Univariate and multivariate analysis of related parameters. Br J Radiol 2020;93:20190891.
29. Takahara T, Imai Y, Yamashita T, Yasuda S, Nasu S, Van Cauteren M. Diffusion weighted whole body imaging with background body signal suppression (DWIBS): technical improvement using free breathing, STIR and high resolution 3D display. Radiat Med 2004;22:275-82.
30. Mosavi F, Laurell A, Ahlström H. Whole body MRI, including diffusion-weighted imaging in follow-up of patients with testicular cancer. Acta Oncol 2015;54:1763-9.
31. Joshi A, Kulkarni S, Dedhia T, Vaswani A. Role of 3T MRI in Evaluation of Bone Marrow Changes in Spine in Various Diseases. J Assoc Physicians India 2019;67:46-51.
32. Niu J, Feng G, Kong X, Wang J, Han P. Age-related marrow conversion and developing epiphysis in the proximal femur: evaluation with STIR MR imaging. J Huazhong Univ Sci Technolog Med Sci 2007;27:617-21.
33. Hawighorst H, Libicher M, Knopp MV, Moehler T, Kauffmann GW, Kaick Gv. Evaluation of angiogenesis and perfusion of bone marrow lesions: role of semiquantitative and quantitative dynamic MRI. J Magn Reson Imaging 1999;10:286-94.

Cite this article as: Bao H, He X, Li X, Cao Y, Zhang N. Magnetic resonance imaging study of normal cranial bone marrow conversion at high altitude. Quant Imaging Med Surg 2022;12(6):3126-3137. doi: 10.21037/qims-21-740

© Quantitative Imaging in Medicine and Surgery. All rights reserved.